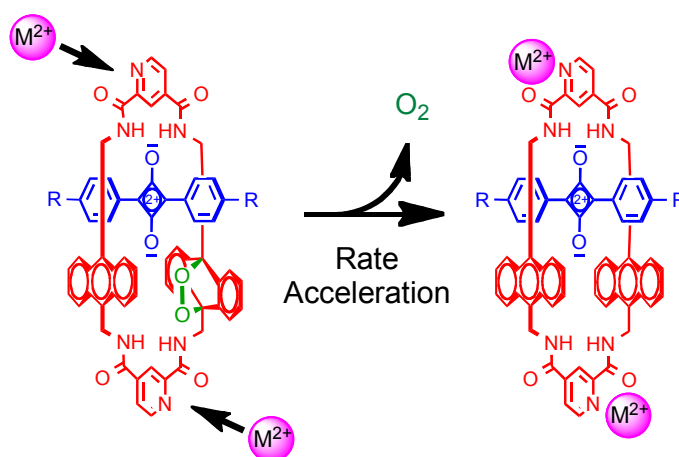


Allosteric regulation of a reactive squaraine rotaxane endoperoxide

Jeffrey M. Baumes, Ivan Murgu, Richard D. Connell, William J. Culligan, Allen G. Oliver and
Bradley D. Smith*

Department of Chemistry and Biochemistry, University of Notre
Dame, Notre Dame, IN, 46556, USA

*email: smith.115@nd.edu



Abstract

Squaraine rotaxane endoperoxides are known to undergo a cycloreversion reaction that is sensitive to the cross-component strain within the interlocked molecules. Two new squaraine rotaxane endoperoxides are described with structures containing metal cation chelation sites that are distal to the reaction center. Fluorescence and absorption titration studies in CH_3CN prove that the metal cations bind to the chelation sites. In one case, the binding of dinuclear metal cations such as $\text{Zn}(\text{II})$ increases the rate of cycloreversion by a factor of four, whereas in the second case, metal cation binding decreases the rate by factor of two.

Keywords: Rotaxane, chelation, allosteric receptor, metal cation complexation, oxygen

1. Introduction

For several decades, supramolecular chemists have explored synthetic models of allosteric regulation.¹ A common approach is to design a host molecule with two separate binding sites and show how binding at one site induces a host conformational change that alters affinity at the second site.² There are also reports of synthetic allosteric systems with a reaction center that is regulated by a distal binding event.³ One of the best known examples uses metal cation binding to force host molecules containing 2,2'-bipyridine units to adopt *syn* conformations that place two reactive sites in close proximity.⁴ Recent advances have moved the field towards allosteric control of coordination assemblies that can be activated to act as synthetic catalysts.⁵ The focus of this report is on rotaxanes, interlocked molecules that have a dumbbell shaped thread component permanently encapsulated inside a macrocycle. The forced proximity of the interlocked components and inherent ability to act as molecular shuttles suggests that rotaxanes have considerable potential to exhibit allosteric behavior. Indeed, several published studies have demonstrated that rotaxane shuttling behavior can be modulated by intermolecular binding events, however, there seems to be no examples showing allosteric control of a chemically reactive rotaxane.^{6, 7}

As part of a program to develop squaraine rotaxanes as high performance dyes for optical imaging applications, we have investigated the chemistry of squaraine rotaxanes with anthracene-containing macrocycles.⁸ This work has uncovered a technically simple photochemical method to prepare squaraine rotaxane endoperoxides such as **1EP**. These unstable compounds can be stored at low temperature but upon warming to body temperature they undergo a cycloreversion reaction that releases singlet oxygen and emits near-infrared light (Fig. 1).⁹ Typically, cycloreversion reactions are not observed with 9,10-dialkylsubstituted anthracene endoperoxides, but the process is facile in the case of endoperoxide **1EP** because the mechanical bond induces cross-component strain on the inwardly directed endoperoxide group.¹⁰ Moreover, we have uncovered structural features that increase the strain and thus accelerate the reaction.¹¹ The most effective method is to employ rotaxanes with a surrounding macrocycle that is wrapped tightly around the encapsulated dye, an effect that produces several hundred-fold rate acceleration. This knowledge has led us to investigate potential allosteric squaraine rotaxane endoperoxides with effector binding sites that are distal to the reaction center. Our supramolecular strategy is to induce a change in rotaxane co-conformation or cross-component

steric strain and thus alter the rate of endoperoxide cycloreversion. The long-term aspiration is to develop switchable squaraine rotaxane endoperoxides that can be maintained in an activated chemical state until triggered by the binding or release of effectors to liberate singlet oxygen and emit light.

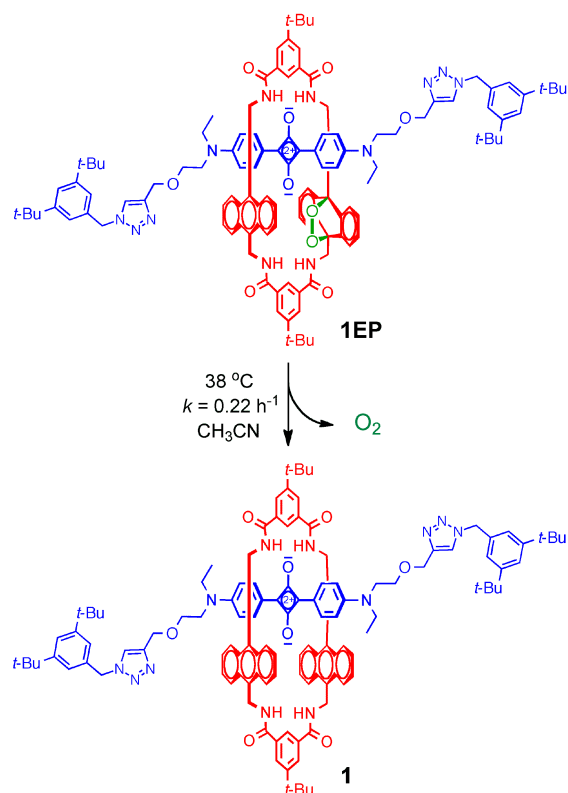


Figure 1. Thermal cycloreversion of squaraine rotaxane endoperoxide, **1EP**.

Here, we describe two squaraine rotaxane endoperoxides, **2EP** and **3EP**, that have binding sites for metal cations as indicated in Figure 2. The first structure, **2EP**, has a surrounding macrocycle with two bridging 2,4-pyridine dicarboxamide units. We reasoned that the pyridyl nitrogen and adjacent carbonyl group would form a putative chelation site for a metal cation, and that cation complexation would tighten the non-covalent grip of the surrounding macrocycle around the encapsulated squaraine and accelerate the rate of cycloreversion.¹² The second structure, **3EP**, has a metal-binding dipicolylamine group attached directly to the

squaraine chromophore, and we wondered if association of a metal cation would alter cross-component strain on the mechanically linked anthracene endoperoxide. We report spectroscopic evidence that metal binding does occur at the chelation sites that are illustrated in Figure 2. In addition, kinetic studies show that these binding events have opposing effects on the cycloreversion reaction. In the case of **2EP** there is a 4-fold rate acceleration, whereas metal binding to **3EP** results in a 2-fold decrease in the rate.

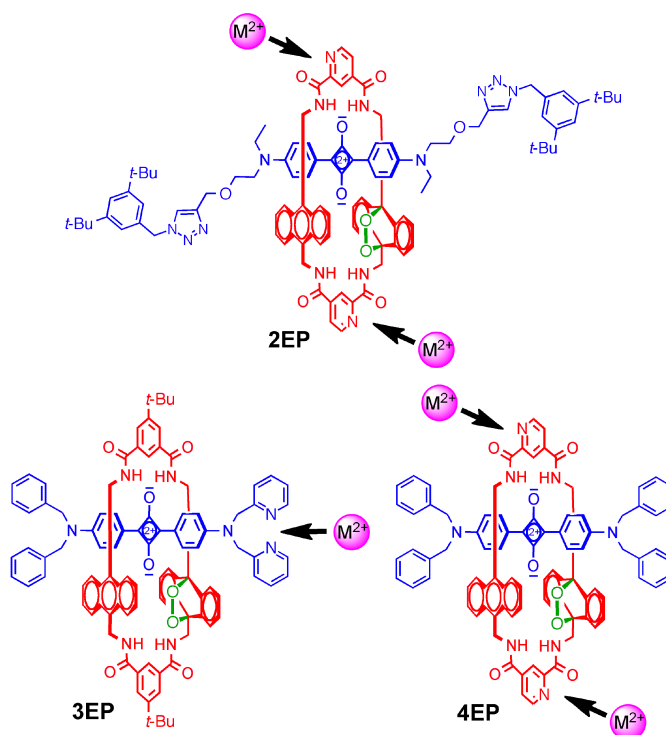


Figure 2. Squaraine rotaxane endoperoxides and their respective metal cation chelation sites.

2. Results and Discussion

2.1 Synthesis and molecular structure

The syntheses and structures of squaraine rotaxane endoperoxides, **1EP** and **3EP**, have been reported previously.^{9,11} The precursors of endoperoxides **2EP** and **4EP**, namely rotaxanes **2** and **4** (Fig. 3), were prepared in yields of 13 % and 28 %, respectively, by reacting two molar equivalents of 9,10-bis(aminomethyl)anthracene and 2,4-pyridinedicarbonyl dichloride in the presence of the appropriate squaraine dye. The rotaxanes were converted to **2EP** and **4EP** in quantitative yield by simply irradiating samples of the parent rotaxanes in aerated CDCl_3 and

monitoring the photooxidation by NMR spectroscopy. Endoperoxide **4EP** was not sufficiently soluble for kinetic studies, but the parent rotaxane **4** was useful because it formed single crystals that were suitable for analysis by X-ray diffraction. Shown in Figure 4 are two views of the molecular structure. The configuration of the tetralactam component is depicted with the two pyridyl nitrogen atoms in an *anti* relationship, however, the diffraction analysis indicates that the *syn* isomer is also present.¹³ The structure shows that each pyridyl nitrogen and adjacent carbonyl combine to form a pre-organized metal chelation site, with minor adjustments of the associated dihedral and bond angles to minimize the inherent lone pair repulsions. The energetic cost of these lone pair repulsions is compensated by the four bifurcated hydrogen bonds between the tetralactam amide NH residues and the squaraine dye oxygen atoms with standard hydrogen bond distances of 2.13 – 2.15 Å as well as N-H...O angles of 167 – 170°.¹⁴ The tetralactam adopts a macrocyclic chair conformation, with a centroid-to-centroid distance of 7.00 Å between the two anthracene walls - a cavity size that is quite similar to previously published anthracene-containing squaraine rotaxanes with isophthalamide bridges.¹⁵ We infer that the co-conformation of rotaxane **2** is analogous to **4** because their ¹H NMR spectra exhibit the same chemical shift shielding trends.

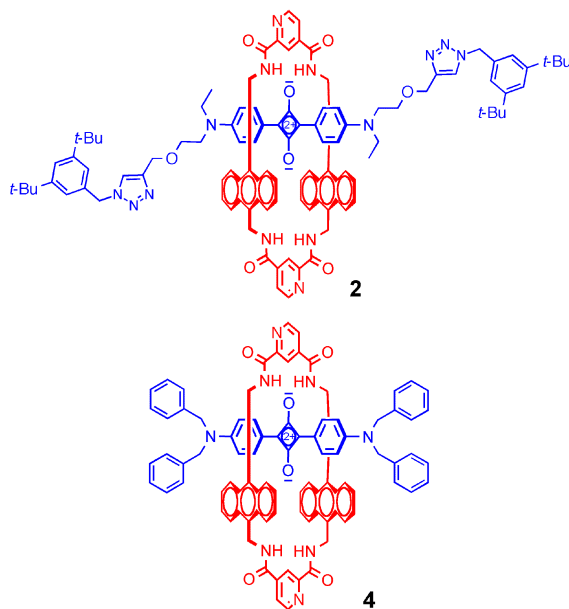


Figure 3. Squaraine rotaxanes **2** and **4**.

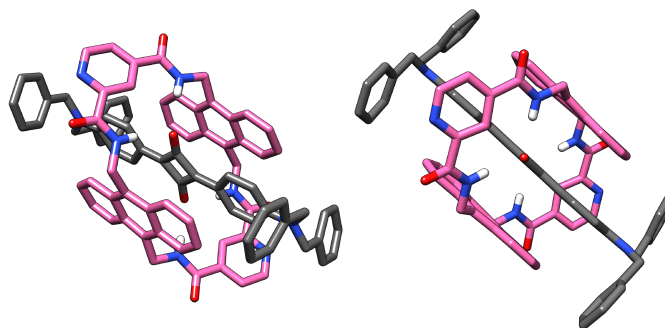


Figure 4. Two different views of the X-ray crystal structure of squaraine rotaxane **4**.

2.2 Metal cation binding

Association of squaraine rotaxane endoperoxides **1EP**, **2EP**, and **3EP** with metal cations in CH_3CN was detected by changes in absorption and fluorescence spectra. Stock solutions containing Zn^{2+} , Ni^{2+} , or Co^{2+} were added to separate solutions containing one of the rotaxane endoperoxides ($5\ \mu\text{M}$), and in each case, the addition of metal cation induced the same spectroscopic effect. With endoperoxide **1EP** additions of up to ten molar equivalents of metal cation produced no significant spectral change (data not shown), indicating no association. With squaraine rotaxane endoperoxide **2EP** there was very little change in the absorption spectrum, but there was significant quenching of the fluorescence emission, as shown by the representative Zn^{2+} results in Fig. 5a and 5b. This outcome is consistent with association of metal cation to the two chelation sites on the surrounding tetralactam (Fig. 2).¹⁶ The binding event does not alter the electronic structure of the encapsulated squaraine dye, which is why there is no change in squaraine absorption. But it does activate fluorescence quenching, because the surrounding tetralactam becomes an electron deficient pyridyl-metal cation complex that can deactivate the encapsulated squaraine excited-state by promoting photoinduced electron transfer (PET).¹⁷ With squaraine rotaxane endoperoxide **3EP**, the addition of metal cation induced both a large blue-shift in the squaraine absorption band and substantial fluorescence quenching, as shown by the representative Zn^{2+} results in Fig. 5c and 5d.¹⁶ These spectral changes are very similar to previous literature observations of related metal cation binding squaraine dyes, and strongly

suggest that the metal cation forms coordination bonds with the dipicolylamine group and also with the adjacent squaraine nitrogen.¹⁸ It is not clear, from the spectroscopic evidence in hand, if the coordinated metal cation also interacts with the macrocycle endoperoxide group in **3EP**, but the small kinetic effect (see below) suggests that it does not. In summary, there is strong spectroscopic evidence that endoperoxides **2EP** and **3EP** associate with Zn^{2+} , Ni^{2+} , and Co^{2+} at the chelation sites that are shown in Fig. 2.

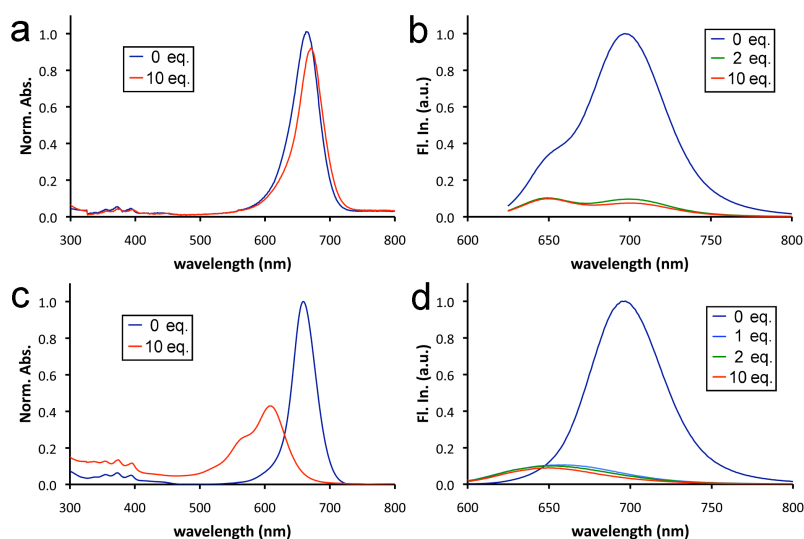


Figure 5. Changes in: (a) absorption and (b) emission spectra of rotaxane **2EP** (5 μM); (c) absorption and (d) emission spectra of rotaxane **3EP** (5 μM), upon addition of 1, 2, or 10 molar equivalents of $\text{Zn}(\text{ClO}_4)_2$ in CH_3CN and 22 °C. Essentially identical results were obtained using $\text{Ni}(\text{ClO}_4)_2$ or $\text{Co}(\text{ClO}_4)_2$.

A unique feature of the cycloreversion reaction for squaraine rotaxane endoperoxides is that it releases singlet oxygen and emits near-infrared light (Fig. 1). The mechanistic evidence in hand indicates that the light is emitted from the excited singlet state of the encapsulated squaraine dye, which is excited by energy transfer from the released singlet oxygen.⁹ Since binding of the dinuclear metal cations leads to fluorescence quenching, it was not surprising to observe that the metal cations also quenched the chemiluminescence of **2EP** and **3EP**.

2.3 Effect of metal cations on the rates of cycloreversion

The rates of cycloreversion for anthracene-9,10-endoperoxides are conveniently measured by monitoring the recovery of the anthracene absorption band at 374 nm.¹⁹ Shown in Fig. 6 are first-order kinetic plots for the cycloreversion of **1EP**, **2EP**, and **3EP** in CH₃CN and 38 °C (chosen to mimic body temperature). The plots also show the kinetic effect that is induced by the presence of Zn²⁺, Ni²⁺, and Co²⁺ and the rate constants derived from this data are listed in Table 1.²⁰ The metal cations have no effect on the cycloreversion of **1EP**, which is expected since the cations do not associate strongly with **1EP**. In the case of **2EP** there is a moderate rate acceleration effect in the relative order of Ni²⁺ (1.5) < Co²⁺ (1.7) < Zn²⁺ (3.9). We postulate that metal cation binding to the external chelation sites on the tetralactam induces tighter wrapping of the macrocycle around the encapsulated dye, which raises cross-component mechanical strain on the internal endoperoxide group and increases the rate of cycloreversion. In the case of **3EP** the presence of metal cation has a modest rate inhibition effect and the relative order of rate constants is Ni²⁺ (0.5) < Co²⁺ (0.6) < Zn²⁺ (0.7). It is not possible to unambiguously assign an energetic reason for this small kinetic change. Empirically, it is interesting that the same metal cations can have opposing effects on cycloreversion rates; that is, they increase the reactivity of **2EP** but decrease the reactivity of **3EP**. This outcome raises the idea of more sophisticated, next-generation allosteric squaraine rotaxane endoperoxides that are equipped with multiple, non-identical effector binding sites, each with their own regulatory effect on the cycloreversion process. However, it must be remembered that binding of dinuclear metal cations leads to quenching of squaraine rotaxane endoperoxide luminescence. Thus, if the functional goal is to trigger an increase in chemiluminescence, effector-activated systems like **2EP** will not be effective even though metal cation binding increases the rate of cycloreversion. A more feasible approach would be to develop analogues of **3EP** that are maintained by metal cation in a low reactivity and weakly luminescent state, with an increase in chemiluminescence triggered by the release of quenching metal cation and concomitant allosteric acceleration of the cycloreversion reaction.

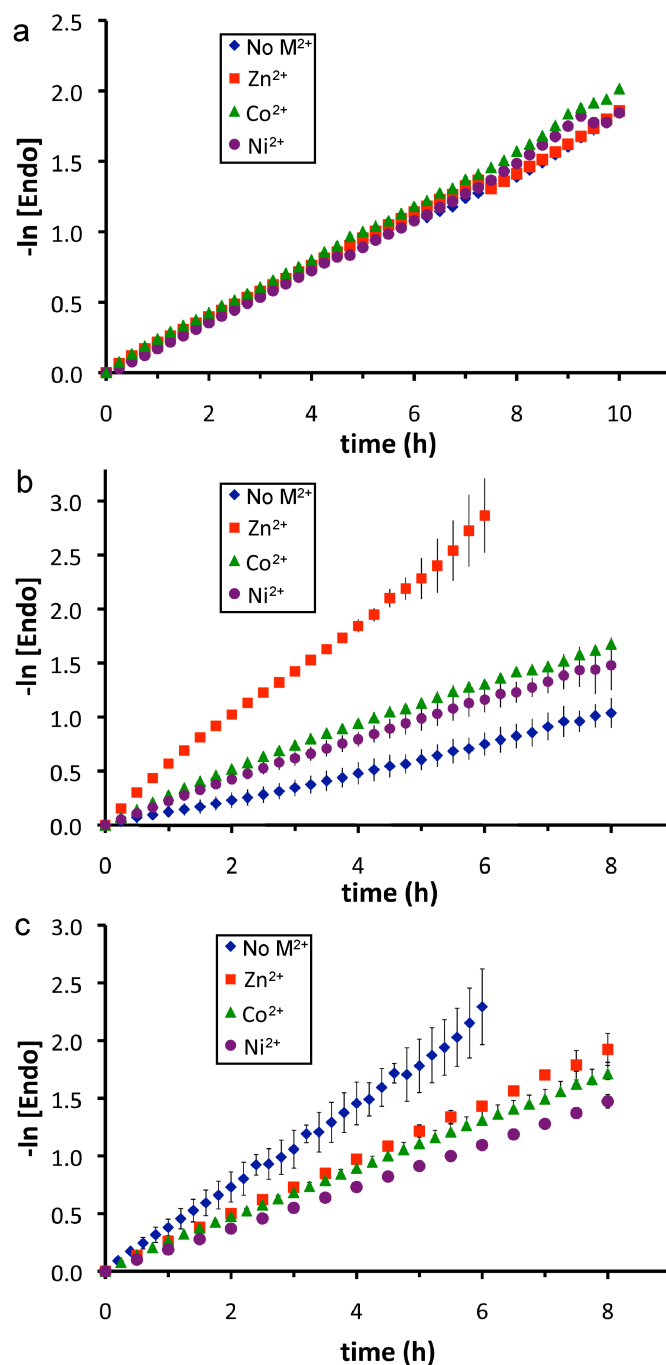


Figure 6. First-order kinetic plots for cycloreversion of; (a) **1EP** ($50 \mu\text{M}$), (b) **2EP** ($50 \mu\text{M}$), and (c) **3EP** ($50 \mu\text{M}$) in the presence of two molar equivalents of metal perchlorate in CH_3CN at 38°C . With **3EP**, twenty molar equivalents of $\text{Co}(\text{ClO}_4)_2$ were added to compensate for lower binding affinity.

Table 1. Cycloreversion rate constants. ^a

Compound	M ²⁺	<i>k</i> (h ⁻¹)	t _{1/2} (h)	<i>k</i> _{rel} ^c
1EP	-	0.22±0.01	3.2±0.1	-
	Ni ²⁺	0.22±0.02	3.1±0.2	1.03
	Co ²⁺	0.24±0.01	2.9±0.1	1.12
	Zn ²⁺	0.23±0.01	3.1±0.1	1.02
2EP	-	0.12±0.02	5.6±0.9	-
	Ni ²⁺	0.19±0.02	3.6±0.5	1.54
	Co ²⁺	0.21±0.01	3.3±0.2	1.72
	Zn ²⁺	0.48±0.01	1.4±0.3	3.89
3EP	-	0.36±0.05	1.9±0.2	-
	Ni ²⁺	0.19±0.01	3.8±0.2	0.50
	Co ^{2+b}	0.22±0.01	3.2±0.1	0.58
	Zn ²⁺	0.24±0.01	2.9±0.1	0.67

^a In CH₃CN at 38 °C with two molar equivalents of perchlorate salt unless stated otherwise.

^b Twenty molar equivalents of Co(ClO₄)₂ were added to compensate for lower binding affinity.

^c Relative to the rate constant in the absence of metal perchlorate.

3. Conclusion

Squaraine rotaxane endoperoxides undergo a spontaneous cycloreversion reaction that releases singlet oxygen and emits near-infrared light (Fig. 1). The structures of **2EP** and **3EP** have different chelation sites for metal cations that are distal from the reaction center (Fig. 2) and metal cation binding induces opposing allosteric behaviour. The rate of cycloreversion for **2EP** is accelerated by a factor of four, whereas, the cycloreversion for **3EP** is decreased by a factor of two. It should be possible to modify these molecular designs and produce more effective

allosteric squaraine rotaxane endoperoxides that can be maintained in their activated chemical state until triggered by the binding or release of effectors.

4. Experimental Section

4.1 General

Thin layer chromatography (TLC) was performed on silica gel 60 F254 (E. Merck). Column chromatography was performed on silica gel (Natland International Corporation, 230-400 mesh) or on SuperFlash Si 35 pre-packed columns (Varian). Kinetic measurements were performed using a temperature controlled Lambda25 (PerkinElmer) absorption spectrometer and seal-capped vials. Chemiluminescence was measured using an IVIS Lumina imaging station (Caliper Life Sciences). Absorption and fluorescence experiments employed spectrophotometric grade solvents (Aldrich). Other reagents and chemicals were purchased from commercial suppliers and used without further purification. The metal salts were hydrated perchlorates (Aldrich).

4.2 Synthesis of squaraine rotaxanes

Squaraine rotaxane endoperoxides **1EP** and **3EP** and the squaraine dyes within **2** and **4** were synthesized according to previously published procedures.^{11, 21}

4.2.1 Generalized clipping procedure for the synthesis of squaraine rotaxanes.

A solution of 2,4-pyridinedicarbonyl dichloride (84 mg, 0.41 mmol) and anhydrous chloroform (30 mL) was drawn up into a 100 mL syringe. A separate solution comprised of the corresponding 9,10-bis(aminomethyl)anthracene (97 mg, 0.41 mmol) and triethylamine (0.30 mL, 2.2 mmol) in anhydrous chloroform (30 mL) was drawn into a separate 100 mL syringe. Over 8 h these solutions were simultaneously added dropwise by a mechanical syringe pump (kd Scientific) apparatus into a stirred solution containing the squaraine dye (0.041 mmol) in anhydrous chloroform (20 mL). After stirring overnight, the reaction was filtered through a pad of Celite to remove any polymeric material. Solvent was removed under reduced pressure and the crude product was purified by column chromatography using silica gel.

4.2.2 Squaraine rotaxane **2**

(Yield 13 %); eluent: CHCl₃:MeOH (100:3); λ_{abs} (CHCl₃) = 665 nm; $\log \epsilon$ (CHCl₃) = 5.10 M⁻¹·cm⁻¹; λ_{em} (CHCl₃) = 695 nm; Φ_{f} (CHCl₃) = 0.43; ¹H NMR (600 MHz, CDCl₃) δ : 9.50 (s, 2H), 9.15 (d, J = 5.0 Hz, 2H), 8.42 (t, J = 4.0 Hz, 2H), 8.26 (dd, J = 5.0 Hz, J = 1.5 Hz, 2H), 8.23 (t, J = 4.0 Hz, 2H), 7.74 (dd, J = 7.0 Hz, J = 3.5 Hz, 4H), 7.71 (dd, J = 7.0 Hz, J = 3.5 Hz, 4H), 7.53 (s, 2H), 7.41 (t, J = 2.0 Hz, 2H), 7.09 (d, J = 2.0 Hz, 4H), 6.89 (d, J = 9.0 Hz, 4H), 6.70–6.63 (m, 8H), 6.14 (d, J = 9.0 Hz, 4H), 5.49 (s, 4H), 5.26 (dd, J = 31 Hz, J = 3.5 Hz, 8H), 4.72 (s, 4H), 3.81 (t, J = 5.5 Hz, 4H), 3.66 (t, J = 6.0 Hz, 4H), 3.56 (q, J = 7.5 Hz, 4H), 1.28 (s, 36H), 1.25 (t, J = 3.5 Hz, 6H); ¹³C NMR (150 MHz, CDCl₃) δ : 12.8, 29.9, 31.6, 35.1, 38.4, 38.5, 46.6, 50.6, 55.1, 64.8, 68.1, 111.9, 117.1, 120.0, 122.7, 122.9, 123.1, 123.9, 124.0, 124.1, 124.2, 124.8, 126.1, 126.2, 128.1, 128.3, 128.5, 128.7, 130.6, 130.7, 133.0, 133.8, 142.1, 144.6, 151.7, 151.9, 152.1, 153.5, 165.3, 165.5, 178.4, 184.5; HRMS (ESI-TOF) calculated for C₁₀₆H₁₁₃N₁₄O₈ [M+H]⁺ 1709.8860; found 1709.8869.

4.2.3 Squaraine rotaxane 4

(Yield 29 %); eluent: CHCl₃:MeOH (100:1); λ_{abs} (CHCl₃) = 660 nm; $\log \epsilon$ (CHCl₃) = 5.18 M⁻¹·cm⁻¹; λ_{em} (CHCl₃) = 694 nm; Φ_{f} (CHCl₃) = 0.46; ¹H NMR (600 MHz, CDCl₃) δ : 9.50 (s, 2H), 9.13 (s, 2H), 8.34 – 8.29 (m, 2H), 8.23 – 8.17 (m, 4H), 7.70 – 7.58 (m, 8H), 7.51 (t, J = 7.5 Hz, 8H), 7.43 (t, J = 7.5 Hz, 4H), 7.30 (d, J = 7.5 Hz, 8H), 6.76 (d, J = 8.5 Hz, 4H), 6.58 – 6.50 (m, 8H), 6.23 (d, J = 8.5 Hz, 4H), 5.26 – 5.22 (m, 4H), 5.18 – 5.15 (m, 4H), 4.87 (s, 8H); ¹³C NMR (150 MHz, CDCl₃) δ : 184.1, 180.1, 165.4, 165.2, 154.7, 151.8, 151.7, 142.1, 136.0, 133.4, 130.6, 130.5, 129.6, 128.7, 128.4, 128.2, 128.0, 126.5, 126.3, 126.2, 124.6, 124.1, 124.0, 123.9, 123.8, 119.9, 117.5, 112.8, 55.5, 38.6, 38.4, 29.9; HRMS (ESI-TOF) calculated for C₉₀H₇₁N₈O₆ [M+H]⁺ 1359.5491; found 1359.5478.

4.3.1. Synthesis of **2EP**

A solution of rotaxane **2** was prepared in CDCl₃ (0.6 mL). The sample was placed approximately 5 cm in front of a 150 W Xenon arc lamp (longpass 520 nm filter) and irradiated for 1 to 2 hrs. Quantitative conversion to **2EP** was verified using ¹H NMR spectroscopy and sample was used without further purification. ¹H NMR (600 MHz, CDCl₃) δ : 9.32 (br s), 9.28 (br s), 9.24 (s), 9.15-9.13 (m), 9.11 (d, J = 5.0 Hz), 8.90 (t, J = 5.0 Hz), 8.85 (t, J = 4.5 Hz), 8.56 (t, J = 4.5 Hz), 8.50 (t, J = 5.0 Hz), 8.32-8.30 (m), 8.19-8.17 (m), 7.85-7.82 (m), 7.80 (dd, J = 7.0 Hz, J = 3.5

Hz), 7.49 (s), 7.42-7.39 (m), 7.15-7.13 (m), 7.11-7.07 (m), 6.77-6.74 (m), 6.48 (dd, $J = 5.5$ Hz, $J = 3.0$ Hz), 6.45-6.43 (m), 6.20 (t, $J = 8.5$ Hz), 6.14 (d, $J = 9.5$ Hz), 5.50-5.39 (m), 4.69 (s), 4.30 (d, $J = 5.0$ Hz), 4.23 (d, $J = 4.0$ Hz), 3.84-3.81 (m), 3.68-3.64 (m), 3.56-3.53 (m), 1.30-1.24 (m).

4.4 X-ray diffraction analysis of rotaxane 4

Rotaxane **4** crystallized as red/green dichroic rod-like crystals from chloroform. The solvent is disordered, not in a well-defined location, and the unit cell contains approximately six molecules of chloroform. SQUEEZE analysis was performed on the data to remove the solvent contribution. The two pyridyl units within the surrounding tetralactam exhibit disorder with respect to the pyridyl nitrogen atom (N3) and its meta carbon (C29). The two sites were modeled as partially occupied and the overall occupancy summed to unity. The Fourier difference map provided further evidence that the two sites were mixed. Two candidate difference peaks were observed at likely positions to be hydrogen atoms indicating that the structure exists with the tetralactam as a mixture of *syn* and *anti* isomers. Additional details for this structure can be found in the crystallographic identification file CCDC-828999 which can be retrieved from the Cambridge Crystallographic Data Centre via www.ccdc.cam.ac.uk/data_request/cif.

4.4.1 Selected crystallographic parameters

Crystal data for $C_{91.50}H_{71.50}Cl_{4.50}N_6O_8$; $M_r = 1542.57$; monoclinic; space group $P2_1/c$; $a = 11.3847(4)$ Å; $b = 17.1607(7)$ Å; $c = 20.4584(8)$ Å; $\alpha = 90^\circ$; $\beta = 101.216(2)^\circ$; $\gamma = 90^\circ$; $V = 3920.6(3)$ Å³; $Z = 2$; $T = 100(2)$ K; $\lambda(\text{Mo-K}\alpha) = 0.71073$ Å; $\mu(\text{Mo-K}\alpha) = 0.231$ mm⁻¹; $d_{\text{calc}} = 1.307$ g.cm⁻³; 46657 reflections collected; 6910 unique ($R_{\text{int}} = 0.0355$); giving $R_1 = 0.0864$, $wR_2 = 0.2289$ for 5854 data with $[I > 2\sigma(I)]$ and $R_1 = 0.0947$, $wR_2 = 0.2334$ for all 6910 data. Residual electron density ($e^- \cdot \text{Å}^{-3}$) max/min: 0.340/-0.449.

4.5 Kinetic measurements

CH₃CN solutions of squaraine rotaxane endoperoxides (50 μM) in seal-capped vials at 38 °C were prepared in the presence or absence of metal perchlorates. Regeneration of the anthracene absorption at 374 nm was monitored every 15 min over a 6-24 h time period. First-order kinetic plots provided rate constants for the cycloreversion reaction.

Acknowledgements

This work was supported by the University of Notre Dame, the Notre Dame Integrated Imaging Facility, and the NSF.

References

- ¹ Kovbasyuk, L.; Krämer, R. *Chem. Rev.* **2004**, *104*, 3161-3187.
- ² (a) Shinkai, S.; Ikeda, M.; Sugasaki, A.; Takeuchi, M. *Acc. Chem. Res.* **2001**, *34*, 494-503. (b) Rebek, J.; Costello, T.; Marshall, L.; Wattley, R.; Gadwood, R. C.; Onan, K. *J. Am. Chem. Soc.* **1985**, *107*, 7481-7487. (c) Onan, K.; Rebek, J.; Costello, T.; Marshall, L. *J. Am. Chem. Soc.* **1983**, *105*, 6759-6760. (d) Rebek, J.; Wattley, R. V.; Costello, T.; Gadwood, R.; Marshall, L. *J. Am. Chem. Soc.* **1980**, *102*, 7398-7400. (e) Ikeda, M.; Kubo, Y.; Yamashita, K.; Ikeda, T.; Takeuchi, M.; Shinkai, S. *Eur. J. Org. Chem.* **2007**, 1883-1886. (f) Hirata, O.; Takeuchi, M.; Shinkai, S. *Chem. Commun.* **2005**, 3805-3807.
- ³ (a) Wakabayashi, R.; Kubo, Y.; Hirata, O.; Takeuchi, M.; Shinkai, S. *Chem. Commun.* **2005**, 5742-5744. (b) Clayton, H. J.; Harding, L. P.; Irvine, J. P.; Jeffery, J. C.; Riis-Johannessen, T.; Laws, A. P.; Rice, C. R.; Whitehead, M. *Chem. Commun.* **2008**, 108-110.
- ⁴ (a) Staats, H.; Lützen, A. *Beilstein J. Org. Chem.* **2010**, *6*, No. 10, doi: 10.3762/bjoc.6.10. (b) Rebek, J.; Costello, T.; Wattley, R. *J. Am. Chem. Soc.* **1985**, *107*, 7487-7493. (c) Rebek, J. *Acc. Chem. Res.* **1984**, *17*, 258-264. (d) Rebek, J.; Marshall, L. *J. Am. Chem. Soc.* **1983**, *105*, 6668-6670. (e) Rebek, J.; Trend, J. E.; Wattley, R. V.; Chakravorti, S. *J. Am. Chem. Soc.* **1979**, *101*, 4333-4337. (f) Rebek, J.; Trend, J. E. *J. Am. Chem. Soc.* **1978**, *100*, 4315-4316.
- ⁵ Wiester, M. J.; Ulmann, P. A.; Mirkin, C. A. *Angew. Chem. Int. Ed.* **2011**, *50*, 114-137.
- ⁶ For allosteric shuttling in rotaxanes, see: (a) Marlin, D. S.; Cabrera, D. G.; Leigh, D. A.; Slawin, A. M. Z. *Angew. Chem. Int. Ed.* **2006**, *45*, 77-83. (b) Marlin, D. S.; Cabrera, D. G.; Leigh, D. A.; Slawin, A. M. Z. *Angew. Chem. Int. Ed.* **2006**, *45*, 1385-1390. (c) Wang, X.; Zhu, J.; Smithrud, D. B. *J. Org. Chem.* **2010**, *75*, 3358-3370.
- ⁷ For inclusion complexes exhibiting allosteric behaviour, see: (a) Lu, X.; Masson, E. *Org. Lett.* **2010**, *12*, 2310-2313. (b) Goldup, S. M.; Leigh, D. A.; McGonigal, P. R.; Ronaldson, V. E.; Slawin, A. M. Z. *J. Am. Chem. Soc.* **2010**, *132*, 315-320. (c) Veling, N.; Thomassen, P. J.; Thordarson, P.; Elemans, J. A. A. W.; Nolte, R. J. M.; Rowan, A. E. *Tetrahedron* **2008**, *64*,

-
- 8535-8542. (d) Beer, P. D.; Sambrook, M. R.; Curiel, D. *Chem. Commun.* **2006**, 2105-2117.
- (e) Sambrook, M. R.; Beer, P. D.; Wisner, J. A.; Paul, R. L.; Cowley, A. R.; Szemes, F.; Drew, G. B. *J. Am. Chem. Soc.* **2005**, *127*, 2292-2302. (f) Takeuchi, M.; Imada, T.; Shinkai, S. *Angew. Chem. Int. Ed.* **1998**, *37*, 2096-2099.
- ⁸ Gassensmith, J. J.; Baumes, J. M.; Smith, B. D. *Chem. Commun.* **2009**, 6329-6338.
- ⁹ Baumes, J. M.; Gassensmith, J. J.; Giblin, J.; Lee, J. -J.; White, A. G.; Culligan, W. J.; Leevy, W. M.; Kuno, M.; Smith, B. D. *Nat. Chem.* **2010**, *2*, 1025-1030.
- ¹⁰ (a) Aubry, J. -M.; Pierlot, C.; Rigaudy, J.; Schmidt, R. *Acc. Chem. Res.* **2003**, *36*, 668-675. (b) Schmidt, R.; Brauer, H. -D. *J. Photochem.* **1986**, *34*, 1-12. (c) Gassensmith, J. J.; Baumes, J. M.; Eberhard, J.; Smith, B. D. *Chem. Commun.* **2009**, 2517-2519.
- ¹¹ Baumes, J. M.; Murgu, I.; Oliver, A.; Smith, B. D. *Org. Lett.* **2010**, *12*, 4980-4983.
- ¹² (a) Tâtucu, M.; Rotaru, P.; Râu, I.; Spînu, C.; Kriza, A. *J. Therm. Anal. Calorim.* **2010**, *100*, 1107-1114. (b) Li, Y. -M.; Zhao, X. -W. *Acta Crystallogr., Sect. E: Struct. Rep. Online* **2007**, *63*, m1589-m1590. (c) Sudbrake, C.; Vahrehkamp, H. *Inorganica Chimica Acta* **2001**, *318*, 23-30. (d) Kirson, B. *Isr. J. Chem.* **1970**, *8*, 709-716.
- ¹³ The *syn* and *anti* isomers of **2** and **4** have the same ¹H NMR spectra and no attempt was made to separate them.
- ¹⁴ Fu, N.; Baumes, J. M.; Arunkumar, E.; Noll, B. C.; Smith, B. D. *J. Org. Chem.* **2009**, *74*, 6462-6468.
- ¹⁵ (a) Gassensmith, J. J.; Arunkumar, E.; Barr, L.; Baumes, J. M.; DiVittorio, K.; Johnson, J. R.; Noll, B. C.; Smith, B. D. *J. Am. Chem. Soc.* **2007**, *129*, 15054-15059. (b) Lee, J. -J.; Baumes, J. M.; Connell, R. D.; Oliver, A. G.; Smith, B. D. *Chem. Commun.* **2011**, *47*, 7188-7190.
- ¹⁶ The fluorescence titration curves produced by smaller incremental additions of metal cation to **2EP** in CH₃CN could not be fitted to simple binding models and suggested that the ratio of metal cation to **2EP** in the associated complex changes as the titration progresses from 1:2 to 2:1. In the case of **3EP**, the titrations curve in CH₃CN showed very strong 1:1 binding of Zn²⁺ and Ni²⁺, but weaker affinity for Co²⁺.
- ¹⁷ (a) Liang, K.; Law, K. -Y.; Whitten, D. G. *J. Phys. Chem. B* **1997**, *101*, 540-546. (b) Jose, D. A.; Shukla, A. D.; Ramakrishna, G.; Palit, D. K.; Ghosh, H. N.; Das, A. *J. Phys. Chem. B* **2007**, *111*, 9078-9087. (c) Durgadas, C. V.; Sharma, C. P.; Sreenivasan *Analyst*, **2011**, *136*,

-
- 933-940. (d) Bolletta, F.; Costa, I.; Fabbrizzi, L.; Licchelli, M.; Montalti, M.; Pallavicini, P.; Prodi, L.; Zaccheroni, N. *J. Chem. Soc., Dalton Trans.* **1999**, 1381-1385. (e) Leigh, D. A.; Morales, M. Á.; Pérez, E. M.; Wong, J. K. Y.; Saiz, C. G.; Slawin, A. M. Z.; Carmichael, A. J.; Haddleton, D. M.; Brouwer, A. M.; Buma, W. J.; Wurpel, G. W. H.; Leon, S.; Zerbetto, F. *Angew. Chem. Int. Ed.* **2005**, *44*, 3062-3067.
- ¹⁸ (a) Ros-Lis, J. V.; Martínez-Máñez, R.; Sancenón, F.; Soto, J.; Spieles, M.; Rurack, K. *Chem.–Eur. J.* **2008**, *14*, 10101-10114. (b) Ros-Lis, J. V.; Martínez-Máñez, R.; Rurack, K.; Sancenón, F.; Soto, J.; Spieles, M. *Inorg. Chem.* **2004**, *43*, 5183-5185. (c) Oguz, U.; Akkaya, E. U. *Tetrahedron Lett.* **1998**, *39*, 5857-5860. (d) Akkaya, E. U.; Turkyilmaz, S. *Tetrahedron Lett.* **1997**, *38*, 4513-4516. (e) Das, S.; Thomas, K. G.; Thomas, K. J.; Kamat, P. V.; George, M. V. *J. Phys. Chem.* **1994**, *98*, 9291-9296.
- ¹⁹ (a) Fudickar, W.; Linker, T. *Chem. Commun.* **2008**, 1771-1773. (b) Zehm, D.; Fudickar, W.; Linker, T. *Angew. Chem. Int. Ed.* **2007**, *46*, 7689-7692. (c) Slavětínská, L.; Mosinger, J.; Kubát, P. *J. Photochem. Photobiol., A* **2008**, *195*, 1-9.
- ²⁰ In the absence of metal cation, the cycloreversion rate constants for the three compounds are **2EP** < **1EP** < **3EP** a trend that we have previously attributed to a difference in effective steric size of the rotaxane stopper groups (see ref. 11).
- ²¹ Gassensmith, J. J.; Barr, L.; Baumes, J. M.; Paek, A.; Nguyen, A.; Smith, B. D. *Org. Lett.* **2008**, *10*, 3343-3346.